Image Reconstruction using a 2D M-channel Perfect Reconstruction Filter Bank with an Optimized Adaptive Interpolation Kernel

J.Y. Kim, K.J. Kim, and S.W. Nam
Department of Electronics and Computer Engineering
Hanyang University
Seoul, 133-791, Korea

Abstract: - In this paper, we propose an image reconstruction method utilizing an optimized adaptive interpolation kernel along with a 2D M-channel perfect reconstruction filter bank(M-ch PR-FB) structure. In particular, the proposed approach leads to sharper reconstructed images than a direct conversion, still preserving high frequency components of the original image by employing the subband processing of a 2D M-ch PR-FB. Finally, the image quality improved by the proposed approach is demonstrated by comparing with those of the direct conversion methods using the bicubic and adaptive 2nd Newton interpolation kernels.

Key-Words: - Image reconstruction, M-ch PR-FB, Compactly Supported Sampling Function, Adaptive interpolation, PSO

1. Introduction

Nowadays, advances in digital technologies enable us to communicate digital images and moving pictures in a short time. Those digital images can be displayed through various multimedia devices, and thus a high quality image reconstruction is necessary for those different multimedia devices. In particular, quality of reconstructed images depends on the interpolation methods applied to estimate the value of pixels not existing in the converted low-resolution image. More specifically, the well-known bilinear and bicubic interpolation methods may lead to some problems such as edge blurring and jagged noise. To solve them, a new adaptive interpolation method, based on 2nd order Newton polynomial, was developed recently to deblur edges in a real-time environment [1]. Also, it is known that the sinc-function is the ideal interpolation kernel from Nyquist–Shannon sampling theory point of view. However, it is difficult to employ in practice the ideal interpolation kernel due to some problems related with its practical implementation [2,3]. Hence, it has been required to derive a sampling function of finite length, similar to the sinc-function. For that purpose, a bifluency method by using the fluency theory [4,5] and a reconstruction method using two-variable interpolation functions [6] were reported. Those approaches yield better image quality than the bilinear and the bicubic methods, but the edge blur and jagged noise may still appear. To solve those problems, an adaptive interpolation kernel based approach, deforming the shape of two-variable interpolation kernels as the direction of the edges, was proposed [7], leading to sharper edges. However, the parameters determining the shapes of kernels need to be optimized to obtain better results. Recently, an optimized adaptive interpolation method based on the particle swarm optimization(PSO) was proposed [8].

In this paper, we propose a new image reconstruction method using a 2D M-ch PR-FB along with an optimized adaptive interpolation kernel, where the edge blur and jagged noise can be reduced and the quality of the reconstructed image can be improved, preserving high frequency components of the original image employing the subband processing. This paper is organized as follows: In Section 2, an optimized adaptive interpolation kernel is described. Also, a 2D M-ch PR-FB structure is presented in Section 3. In Section 4, the quality of images reconstructed by the proposed method is compared with those by the direct conversion methods using bicubic and adaptive 2nd Newton interpolation kernels. Finally, the conclusions are made in Section 5.

2. Optimized adaptive interpolation kernel

2.1. Derivation of the compactly supported sampling functions of degree 2

According to the Nyquist–Shannon sampling theorem, bandlimited signals are exactly reconstructed by using the sinc function. This means that the signal is continuously differentiable. Also, it implies that discontinuous signals observed in edges of images can not be reconstructed perfectly by using the sinc function. Therefore, in this section, an optimized adaptive interpolation kernel using a compactly supported sampling function (CSSF) of degree 2 is explained, which is similar to the sinc function and is of finite extent [4]. Furthermore, the sampling function is derived by fluency theory [4, 5] as follows:

$$ {}^{m}_{[b]}\psi_{l}(t) = \int_{-\infty}^{\infty} \left(\frac{\sin \pi f h}{\pi f h} \right)^{m} e^{j2\pi f(t-lh)} df \tag{1} $$

$$ \psi^{3}_{[s],0}(t) = \sum_{\lambda=-2}^{2} b(\lambda)\phi_{3}(t+\frac{3}{2}-\frac{\lambda}{2}) \tag{2} $$

In (1), $\{ {}^{m}_{[b]}\psi_{l} \}_{-\infty}^{\infty}$ are called a B-spline basis of degree (m-1) [5]. and h is a sampling interval. When l is zero, the B-spline basis of degree of 2, ${}^{3}_{[b]}\psi_0(t)$, has a symmetric property with respect to t=0. The compactly supported sampling function of degree of 2, $\psi^3_{[s],0}(t)$ is defined as (2) with coefficients, $\{b(\lambda)\}_{\lambda=-2}^{2}$.

$$\phi_3(t)={}^{3}_{[b]}\psi(t-\frac{3}{2}) \tag{3}$$

$$\phi_1(t)=\begin{Bmatrix}1, & 0\le t\le 1\\ 0, & otherwise\end{Bmatrix},\ \phi_3(t)=\phi_1(t)*\phi_1(t)*\phi_1(t) \tag{4}$$

In (3), a piecewise polynomial of degree 2, $\phi_3(t)$, is obtained by repeating two times convolution of $\phi_1(t)$ which is a piecewise polynomial of degree 1 defined in (4).

$$\phi_3(t)=\sum_{k=0}^{3}\frac{1}{2^2}\binom{3}{k}\phi_3(2t-k) \tag{5}$$

$$\hat{\phi}_3(f)=H_3(e^{j\pi f})\hat{\phi}_3(\frac{f}{2}),\ H_3(e^{j\pi f})=\left(\frac{1+e^{-j\pi f}}{2}\right)^3 \tag{6}$$

$$\psi^3_{[s],0}(t)=\sum_{\lambda=-2}^{2}2a_3(2t-\lambda)b(\lambda),\ a_3(\lambda)=\sum_{k=0}^{3}\frac{1}{2^3}\binom{3}{k}\phi_3(k-\lambda) \tag{7}$$

Also, (5) can be derived by using the relation between Fourier transform $\hat{\phi}_3(f)$ of $\phi_3(t)$ and $\hat{\phi}_3(f/2)$ as in (6). Furthermore, $\psi^3_{[s],0}(t)$ in (7) can be rearranged by substituting (5) into (2).

$$\psi^3_{[s],0}(t)=-\frac{1}{2}\phi_3(t+2)+2\phi_3(t+\frac{3}{2})-\frac{1}{2}\phi_3(t+1) \tag{8}$$

Then, from the necessary condition that $\psi^3_{[s],0}(t)$ becomes a sampling function, $\psi^3_{[s],0}(k)=\delta_k$, each value of $\{b(\lambda)\}_{\lambda=-2}^{2}$ in (2) can be obtained. With these values, one of the compactly supported sampling functions of degree 2 can be derived as (8). By replacing the sinc function presented in [2] with $\psi^3_{[s],0}(t)$, new sampling and interpolation kernels are presented in Table 1. Here, $G(i,j)$ are sampling pixels and $F(x,y)$ are pixels of the output image. $N(x,y)$ consists of pixels in the neighborhood of interpolated pixels where sampling function, $\psi^3_{[s],0}(t)$ is nonzero.

2.2. Adaptive interpolation process

An adaptive process applied to the interpolation kernel by using the compactly supported sampling function of degree 2 can be described as follows [8]:

$$V=\frac{\sum_{k=1}^{8}(d_k-\bar{d})^2}{8},\ \bar{d}=\frac{\sum_{k=1}^{8}d_k}{8} \tag{9}$$

In (9), the variance V of the difference values d_k of each sampling point and its 8 neighborhood pixels is calculated for determining whether each sampling point is near the edge of the original image or not. If V is higher than the threshold V_s, the sampling point is near edge. If each sampling point is near the edge, the adaptive interpolation kernels can be used to calculate the value of the interpolated pixels. On the other hand, the interpolation kernels using CSSF of degree 2 as in Table 1 can be utilized.

$$R_k=\frac{d_k}{G_{\max}}R_{\max} \tag{10}$$

$$E_{a_k}=\frac{D_{\max}-d_k}{D_{\max}}E_{\max} \tag{11}$$

For deforming adaptively the shape of the interpolation kernels, the contraction value R_k and the expansion value E_{a_k} of each axis on the sampling point S_a on Fig. 1 need to be calculated from (10) and (11), respectively. Here, $D_{ma:}$ is the maximal difference value, and $G_{\max}$ is the maximal value of 8 neighborhood pixels. Also, V_s, $R_{\max}$ and $E_{\max}$ are the threshold value, the maximal contraction value, and the maximal expansion value, respectively. In particular, the expansion value E_{a_k} is updated L times to come up to an appropriate value. For example, in case of k=2, E_{a_2} becomes

$$E'_{a_2}=\frac{\sqrt{E_{a_1}E_{b'_2}}+\sqrt{E_{a_2}E_{c'_2}}+\sqrt{E_{a_3}E_{d'_2}}}{3},\ E_{b'_2}=\frac{G_{\max}-|S_a-S_b|}{G_{\max}}E_{b_2} \tag{12}$$

Here, E_{b_2}, E_{c_2} and E_{d_2} are the expansion values of neighbor sampling points S_b, S_c and S_d of S_a on Fig. 1, respectively. Also, $E_{b'_2}, E_{c'_2}$ and $E_{d'_2}$ are the new value of E_{b_2}, E_{c_2} and E_{d_2}.

$$\gamma_k=1-R_k+E_{a_k} \tag{13}$$

$$\gamma_D(\theta,\gamma_k,\gamma_{k+1})=\frac{\gamma_k\gamma_{k+1}}{(\sqrt{2}\gamma_{k+1}-\gamma_k)\sin\theta+\gamma_k\cos\theta} \tag{14}$$

Then, the expansion/contraction rate can be obtained from (13). Finally, the expansion/contraction rates in the direction of the interpolated pixel can be calculated from (14). Here, the interpolated pixel can be placed between the k-th and the (k+1)-th axes of 8 axes. The interpolation kernel in Table 1

Down Sample by "M"	Horizontal (column)	$F(x,y)=\frac{1}{M}\sum_{i,j\in N(x,y)}G(i,j)\psi^3_{[s],0}(x-i)\psi^3_{[s],0}(y-\frac{j}{M})$
	Vertical (row)	$F(x,y)=\frac{1}{M}\sum_{i,j\in N(x,y)}G(i,j)\psi^3_{[s],0}(x-\frac{i}{M})\psi^3_{[s],0}(y-j)$
Up Sample by "M"	Horizontal (column)	$F(x,y)=\sum_{i,j\in N(x,y)}G(i,j)\psi^3_{[s],0}(x-i)\psi^3_{[s],0}(\frac{y}{M}-j)$
	Vertical (row)	$F(x,y)=\sum_{i,j\in N(x,y)}G(i,j)\psi^3_{[s],0}(\frac{x}{M}-i)\psi^3_{[s],0}(y-j)$

Table 1. 2D down-sampling and up-sampling formulas with kernel using CSSF of degree 2

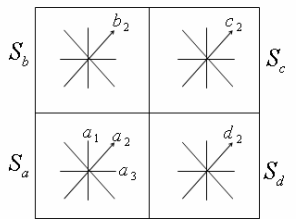

Fig.1. Calculation of the expansion value

is deformed as in Table 2. In particular, the shape of the adaptive interpolation kernel can be changed only in horizontal and vertical directions for the 2D M-ch PR-FB.

Table 2. The adaptive interpolation kernel

Horizontal(column)	$\psi^3_{[s],0}(x,y,i,j)=\psi^3_{[s],0}(x-i)\psi^3_{[s],0}((\frac{y}{M}-j)/\gamma_D)$
Vertical(row)	$\psi^3_{[s],0}(x,y,i,j)=\psi^3_{[s],0}((\frac{x}{M}-i)/\gamma_D)\psi^3_{[s],0}(y-j)$

2.3. Parameters optimization using PSO

An adaptive interpolation process controls adaptively the influence of pixels near the edge of the original image. However, it is possible to emphasize too strongly or too weakly due to experientially given parameter sets in the approach. Therefore, these parameter sets are required to be optimized for better results. In this section, an optimization method (i.e., particle swarm optimization) [9] for searching parameter sets maximizing PSNR (Peak Signal to Noise Ratio) of reconstructed images in a 2D M-ch PR-FB structure is described. Firstly, arbitrary parameters are preset. In Section 2.2, the parameter sets are V_s, $R_{\max}$, $E_{\max}$ and L, respectively. Next, the low resolution image can be obtained by sampling kernels with M scaling factor as in Table 1. When the image is enlarged to the original size by an interpolation process, it is compared with the original image. If the PSNR is the highest, the parameter sets are stored as the best values. Then this process is repeated for the fixed number of times. Here, the value of the parameter sets are obtained as follows: A particle is an each piece that searches through the predetermined search space. Particles behave according to rules incorporating its individual observation, memory and information shared among the group (swarm). Each particle has positional vectors $\vec{x}$, velocity vectors $\vec{v}$, a memory of its maximally evaluated coordinate $\vec{p}$ and the best solution in the swarm $\vec{g}$. The next search point is obtained by

$$\vec{x}(t+1)=\vec{x}(t)+\vec{v}(t+1) \quad (15)$$

Also, the velocity can be updated as

$$\vec{v}(t+1)=\vec{v}(t)+\lambda_1(\vec{p}-\vec{x})+\lambda_2(\vec{g}-\vec{x}) \quad (16)$$

Here, positive numbers λ_1 and λ_2 are randomly chosen. When the search point $\vec{x}$ is updated, the parameter setting will be tested by PSNR evaluation. After repeating the fixed number of times, optimized parameter sets will be converged to $\vec{g}$.

3. 2D M-ch PR-FB structure

A 2D M-ch PR-FB structure, separated into two directions with sampling and interpolation kernel is presented on Fig. 2. In this paper, the 2D non-uniform 4ch PR-FB with rational or irrational scaling factors proposed in [2] is further utilized for a 2D uniform M-ch PR-FB structure. Thus, scaling factors in each kernel are fixed to M. This structure has very considerable freedom for M>2 and can reduce round- off errors coming from irrational scaling factors. When signals are down-sampled, the signals should be bandlimited by using an anti-aliasing filter before sampling. Here, high frequency components of signals are removed by low pass filtering. Thus, it is impossible to reconstruct perfectly down sampled signals. However, a perfect reconstruction can be obtained by sending high frequency components of the original signal to another channel and synthesizing the decomposed signals through a subband processing in a PR-FB structure. In particular, sampling and interpolation kernels in a closed form are utilized in this paper, instead of designing a pre-filter or a post-filter for down sampling or up sampling, respectively. Sampling kernels and interpolation kernels summarized in Table 1-2 are used in the analysis part and the synthesis part of 2D M-ch PR-FB, respectively. In the 2D M-ch PR-FB, two dimensional images are processed in horizontal and vertical directions, respectively, while still preserving high frequency components through a subband processing for high quality image reconstruction.

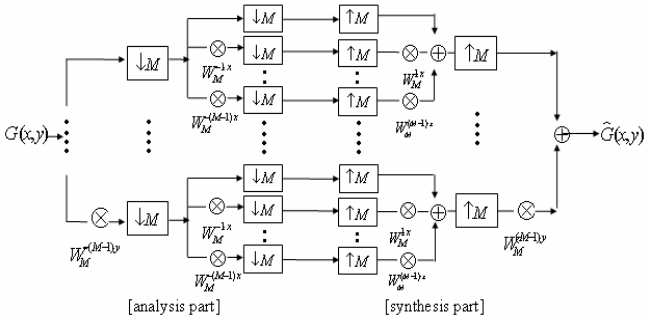

Fig.2. 2D M-ch PR- FB structure

4. Experimental results

In this section, the simulation results are shown. The low resolution images down-sampled by a factor of 2 in horizontal and vertical directions from the original images, are reconstructed by using the bicubic and the adaptive 2nd Newton interpolation methods. Also, the quality of images, reconstructed by the proposed 2D PR-FB structure of 2ch (i.e., a scaling factor is 2) in each direction, is compared with those by the direct conversion methods using the bicubic and adaptive 2nd Newton interpolation kernels. Also, the Peak Signal-to-Noise Ratio (PSNR) can be calculated to evaluate the quality of images, where the PSNR is defined by

$$PSNR=10\log_{10}\frac{MAX_I^2}{MSE},\ MSE=\frac{\sum_{j=1}^{y}\sum_{i=1}^{x}(X'_{ij}-X_{ij})^2}{x\times y} \quad (17)$$

In (17), x, y denote the numbers of rows and columns of the images, respectively. X'_{ij}, X_{ij} are the values of the pixel of reconstructed images and input images at point (i, j), respectively. Also, MAX_I is the maximum value of pixels. In this experiment, the value is fixed to 255 due to using 256 level (0-255) gray-scale images. Images on Fig. 3 were used as the experimental images, the size of which are

64×64 and 256×256. Parameters used in adaptive interpolation kernels are optimized by PSO method described in section 2.3. Optimized parameters, obtained by repeating 100 times PSO method with respect to each image of size 64×64 on Fig. 3 are shown in Table 3. The results obtained by using each reconstruction method are shown in Table 4. PSNR of images reconstructed by the proposed method (2ch) yields the highest. Also, the input images of larger size lead to the higher PSNR.

(a) Barbara (b) Lena (c) Lake

Fig. 3. Original images

Table 3. Optimized parameters of original images

Images	E_{max}	R_{max}	L	V_s
Barbara	-0.0242	-0.0242	1	467.6343
Lena	0.0353	0.0577	1	321.2327
Lake	0.0152	-0.0282	1	371.3845

The zoomed versions of the region specified in the image of 256×256 size and the frequency domain representation of the reconstructed "Barbara" image are shown in Fig. 4(a)-(b). From the results of Fig. 4, we can see that the proposed method (2ch) yields clearer edges, and the frequency domain representation (dB) by the proposed method (2ch) is almost same as that of the original image. Those visual improvement and higher PSNR can be obtained by controlling the influence of pixels near the edges with an optimized adaptive interpolation and by preserving high frequency components of the original image with a 2D PR-FB structure as in Fig. 4(b).

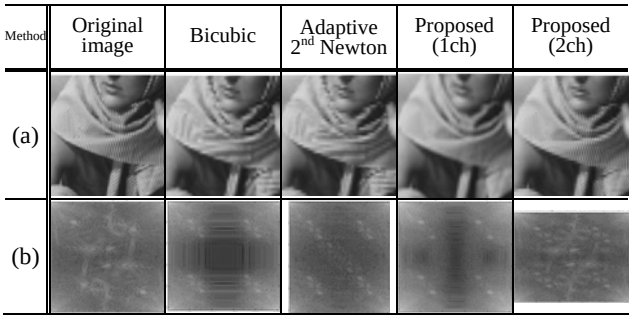

Fig. 4. (a) The zoomed versions and (b) frequency domain representation of the reconstructed "Barbara" image.

5. Conclusions

In this paper, we proposed an image reconstruction method utilizing a 2D M-ch PR-FB with an optimized adaptive interpolation kernel using compactly supported sampling function of degree 2. The experimental results, i.e., images reconstructed by the proposed approach, provide higher PSNR and show clearer edges than the direct conversion methods using the bicubic and adaptive 2nd Newton interpolation methods. Further utilization of the proposed approach for real-time image processing will be further investigated as a future work.

Acknowledgement

This study was supported by a grant of the Korea Health 21 R& D project, Ministry of Health & Welfare, Republic of Korea (02-PJ3-PG6-EV08-0001).

Table 4. Comparison of PSNR of reconstructed images

size	Images	Bicubic	Adaptive 2nd Newton	Proposed (1ch)	Proposed (2ch)
64 × 64	Barbara	21.4295	23.2936	22.3739	23.5111
	Lena	21.4286	23.8055	22.6510	24.1616
	Lake	20.1256	21.6722	21.9369	23.7783
256 × 256	Barbara	25.7046	27.8177	27.2230	28.8821
	Lena	26.4799	29.7575	28.4179	29.8624
	Lake	24.0696	26.2288	26.5107	28.0418

References:

[1] J. Xiao. X. Zo, Z. Liu, and X. Guo, "Adaptive interpolation algorithm for real-time Image resizing," *Proc. of IEEE ICICIC2006*, vol. 2, pp. 221-224, Aug., 2006.

[2] S. C. Pei and M. P. Kao, "Two Dimensional Nonuniform Perfect Reconstruction Filter Bank with Irrational Down-sampling Matrices," *Proc. of ISCAS2005*, vol. 2, pp. 1086-1089, May, 2005.

[3] E.H.W. Meijering, K.J. Zuiderveld, and M.A. Viergever, "Image reconstruction by convolution with symmetrical piecewise nth-order polynomial kernels," *IEEE Trans. Image Processing*, vol. 8, no. 2, pp. 192-201, Feb., 1999.

[4] K. Katagishi, K. Toraichi, K. Hattori, S.L. Lee, and K. Nakamura, "Practical Compactly Supported Sampling Functions of degree 2," *Proc. of IEEE PACRIM. Communications, Computers and signal Processing*, pp. 552-555, Aug., 1999.

[5] K. Katagishi, K. Toraichi, M. Obata and K. Wada, "A practical least squares approximation based on biorthonormal expansions in the signal space of piecewise polynomials," *Trans. IEICE*, vol. 118-C, no. 3, pp. 353-365, 1998.

[6] H. Aokage, K. Wada and K. Toraichi, "High quality conversion of image resolution using two-dimensional sampling function," *Proc. of IEEE PACRIM. Communications, Computers and signal Processing*, vol. 2, pp. 720-723, Aug., 2003.

[7] Y. Ohmiya, K. Katagishi, P.W.H. Kwan, K. Toraichi, A. Matsumura, R. Kawada, A. Koike, and H. Murakami, "A method for high precision enlargement of pictures taken by cellular phone on personal computer," *Proc. of CCCT2004*, pp. 30-35, 2004.

[8] A. Fujii, K. Kameyama, T. Kamina, Y. Ohmiya, and K. Toraichi, "Image resolution conversion by optimized adaptation of interpolation kernels," *Proc. of the 24th IASTED International Multi-Conference Signal Processing, Pattern Recognition, and Applications*, Feb., 2006.

[9] J. Kennedy and R. Eberhart, "Particle Swarm optimization," *Proc. of IEEE ICNN*, vol. 4, pp. 1942-1948, 1995.